Cell Tissue Res (2007) 328:31–47
DOI 10.1007/s00441-006-0324-z

REGULAR ARTICLE

Prominin-2 is a cholesterol-binding protein associated with apical and basolateral plasmalemmal protrusions in polarized epithelial cells and released into urine

Mareike Florek · Nicola Bauer · Peggy Janich · Michaela Wilsch-Braeuninger · Christine A. Fargeas · Anne-Marie Marzesco · Gerhard Ehninger · Christoph Thiele · Wieland B. Huttner · Denis Corbeil

Received: 28 June 2006 / Accepted: 8 August 2006 / Published online: 16 November 2006
© Springer-Verlag 2006

Abstract Prominin-2 is a pentaspan membrane glycoprotein structurally related to the cholesterol-binding protein prominin-1, which is expressed in epithelial and non-epithelial cells. Although prominin-1 expression is widespread throughout the organism, the loss of its function solely causes retinal degeneration. The finding that prominin-2 appears to be restricted to epithelial cells, such as those found in kidney tubules, raises the possibility that prominin-2 functionally substitutes prominin-1 in tissues other than the retina and provokes a search for a definition of its morphological and biochemical characteristics. Here, we have investigated, by using MDCK cells as an epithelial cell model, whether prominin-2 shares the biochemical and morphological properties of prominin-1. Interestingly, we have found that, whereas prominin-2 is not restricted to the apical domain like prominin-1 but is distributed in a non-polarized fashion between the apical and basolateral plasma membranes, it retains the main feature of prominin-1, i.e. its selective concentration in plasmalemmal protrusions; prominin-2 is confined to microvilli, cilia and other acetylated tubulin-positive protruding structures. Similar to prominin-1, prominin-2 is partly associated with detergent-resistant membranes in a cholesterol-dependent manner, suggesting its incorporation into membrane microdomains, and binds directly to plasma membrane cholesterol. Finally, prominin-2 is also associated with small membrane particles that are released into the culture media and found in a physiological fluid, i.e. urine. Together, these data show that all the characteristics of prominin-1 are shared by prominin-2, which is in agreement with a possible redundancy in their role as potential organizers of plasma membrane protrusions.

Keywords Prominin-1 (CD133) · Lipid raft · Microvillus · Prominosome · MDCK cells · Mouse (C57B16)

M.F. and N.B. can be considered as joint first authors.

C.T. was supported by the Deutsche Forschungsgemeinschaft (SFB/TR13-04 D2), W.B.H. by the Deutsche Forschungsgemeinschaft (SPP 1109, Hu 275/7-2; SPP 1111, Hu 275/8-2; SFB/TR13-04 B1; SFB 655 A2) and the Fonds der Chemischen Industrie and D.C. was supported by the Deutsche Forschungsgemeinschaft (SPP 1109, CO 298/2-2; SFB/TR13-04 B1; SFB 655 A13) and the Sächsisches Ministerium für Wissenschaft und Kunst: Europäischer Fond für Regionale Entwicklung (4212/05-16).

N. Bauer · P. Janich · C. A. Fargeas · D. Corbeil (✉)
Tissue Engineering Laboratories, BIOTEC,
Tatzberg 47-51,
01307 Dresden, Germany
e-mail: denis.corbeil@biotec.tu-dresden.de

M. Florek · G. Ehninger
Medical Clinic and Polyclinic I, Technische Universität Dresden,
Fetscherstrasse 74,
01307 Dresden, Germany

M. Wilsch-Braeuninger · A.-M. Marzesco · C. Thiele · W. B. Huttner
Max Planck Institute for Molecular Cell Biology and Genetics,
Pfotenhauerstrasse 108,
01307 Dresden, Germany

Introduction

Prominin-1 (CD133), the first characterized member of a novel family of pentaspan membrane glycoproteins conserved throughout metazoan evolution (Fargeas et al. 2003a,b; Miraglia et al. 1997; Weigmann et al. 1997), binds to plasma membrane cholesterol (Röper et al. 2000) and is selectively associated with plasma membrane

protrusions irrespective of the cell type (for reviews, see Corbeil et al. 2001b; Fargeas et al. 2006). In epithelial cells, prominin-1 is found in microvilli present within the apical plasma membrane domain (Corbeil et al. 1999, 2000; Fargeas et al. 2004; Marzesco et al. 2005; Weigmann et al. 1997), whereas in non-epithelial cells, it is concentrated in various types of plasmalemmal protrusion, such as filopodia (Corbeil et al. 2000; Weigmann et al. 1997) and uropods (Giebel et al. 2004). We have previously demonstrated that the specific localization of prominin-1 in plasma membrane protrusions involves a cholesterol-based membrane microdomain (Röper et al. 2000). Prominin-1 not only is tightly associated with the plasma membrane, but is also released into the extracellular milieu. Specifically, prominin-1 is associated with membrane particles that are found in a variety of body fluids, including urine, saliva and seminal fluids (Marzesco et al. 2005). Although the cellular mechanism underlying the release of these particles, referred to as prominosomes, has not yet been elucidated, the high concentration of prominin-1 at the tip of microvilli (Weigmann et al. 1997) strongly suggests that they are derived from this location.

General interest in prominin-1 has grown rapidly, as it appears to be an important cell-surface marker that can widely be used to identify and isolate stem cells from various sources (Bussolati et al. 2005; Kania et al. 2005; Richardson et al. 2004), including the haematopoietic (Am Esch et al. 2005; Bitan et al. 2005; Bornhäuser et al. 2005) and central nervous systems (Lee et al. 2005; Uchida et al. 2000). The characterization of this molecule has also been stimulated by the identification of a frameshift mutation in the human *PROMININ-1* gene preventing its cell-surface appearance and causing autosomal recessive retinal degeneration (Maw et al. 2000). In keeping with the preferential association of prominin-1 with plasma membrane protrusions, prominin-1 is concentrated in plasma membrane evaginations at the base of the rod outer segments that have an essential role in the biogenesis of photoreceptor disks (Maw et al. 2000). The knockout of mouse prominin-1 leads to the complete disorganization of the outer segment of photoreceptor cells in younger mice and to the entire loss of photoreceptor cells in older animals (Oh et al. 2005). Together, these observations suggest that prominin-1 is involved in the maintenance of functional plasma membrane protrusions (Corbeil et al. 2001b; Jászai et al. 2006).

We have reported the identification of prominin-2, a glycoprotein structurally related to prominin-1 and encoded by a distinct gene (Fargeas et al. 2003b). Although the amino acid identity between prominin-1 and prominin-2 is low (<30%; Corbeil et al. 2001b; Fargeas et al. 2003b), their genomic organization is strikingly similar, suggesting that both *prominin* genes originate from a common ancestral gene (Fargeas et al. 2003b). Like prominin-1, prominin-2 does not show obvious sequence homology to other known proteins, nor does its sequence reveal a motif that could provide clues as to its physiological role. Upon transfection in non-epithelial cells, prominin-2 also becomes concentrated in plasma membrane protrusions (Fargeas et al. 2003b) raising the possibility that prominin-2 exerts a similar function as prominin-1, i.e. by acting as an organizer of certain plasma membrane protrusions. In agreement with this, prominin-2 shows a tissue distribution similar to prominin-1, being highly expressed in the adult kidney and detectable all along the digestive tract and in various other epithelial tissues. However, although prominin-1 is expressed in epithelial and non-epithelial cells (Weigmann et al. 1997; Yin et al. 1997), the tissue distribution of prominin-2 suggests that its expression is restricted to epithelial cells (Fargeas et al. 2003b; Zhang et al. 2002). Prominin-2 might therefore be related to the epithelial features of cells.

In the present study, we have undertaken the cellular and biochemical characterization of prominin-2 in polarized epithelial cells and investigated whether prominin-2, like prominin-1, specifically (1) is localized at the apical domain of epithelial cells, (2) is concentrated in plasma membrane protrusions, (3) is released into extracellular fluids, (4) binds to the plasma membrane cholesterol and (5) is associated with lipid microdomains. Addressing these issues is particularly important because, despite the widespread tissue distribution of prominin-1, patients carrying a prominin-1 mutation do not have obvious pathological signs other than retinal degeneration (Maw et al. 2000), suggesting that prominin-2 functionally substitutes for the lack of prominin-1 in other tissues, which, in contrast to the retina, contain not only prominin-1, but also prominin-2 (Fargeas et al. 2003b).

Materials and methods

Cell culture and transfection

Madin-Darby canine kidney (MDCK) cells (strain II) were maintained in a humidified incubator at 37°C under a 5% CO_2 atmosphere in Eagle's minimal essential medium supplemented with 10% fetal calf serum, 100 IU/ml penicillin and 100 μg/ml streptomycin. MDCK cells either were double-transfected with the eukaryotic expression plasmids pRc/CMV-prominin containing mouse prominin-1 (Weigmann et al. 1997) and pEGFP-N1-rat prominin-2 expressing a fusion protein in which GFP (green fluorescent protein) is fused to the cytoplasmic C-terminal domain of prominin-2 (Fargeas et al. 2003b) or were transfected with the pCMV-mouse-prominin-2 plasmid (Fargeas et al. 2003b) or the pEGFP-N1-rat prominin-2 plasmid alone by using the nucleofection method with solution T and program no. G-16 (Amaxa, Cologne, Germany). The

MDCK cells expressing the neomycin-resistance gene were then selected by adding 600 μg/ml G418 to the culture medium. Two weeks later, G418-resistant colonies were pooled and expanded in the presence of G418. Under these conditions, approximately 20%–40% of stably transfected cells expressed the transgene. To enhance transgene expression, MDCK cells were incubated for 17 h with 5 mM sodium butyrate prior to analysis. For experiments studying the polarized distribution of prominins, transfected MDCK cells were plated at confluency on permeable membranes (0.4 μm pore size) by using either 24-mm Transwell-COL chambers (Costar, Cambridge, Mass.) or 12-mm Corning tissue culture inserts (Corning) and cultured as previously described (Corbeil et al. 1992).

Some transfected cells were then used for cell-surface biotinylation, immunofluorescence and electron microscopy. Others were solubilized in ice-cold solubilization buffer I (1% Triton X-100, 0.1% SDS, 150 mM NaCl, 5 mM EGTA, 50 mM TRIS-HCl, pH 7.5, and protease inhibitor cocktail from Sigma, St. Louis, Mo., USA) and the detergent extract obtained after centrifugation (10 min, 10,000*g*) was used for deglycosylation, SDS-polyacrylamide gel electrophoresis (SDS-PAGE) and immunoblotting assays (see below).

Endoglycosidase digestion and immunoblotting

Detergent extracts of transfected MDCK cells (corresponding to one-fifth of a confluent 100-mm dish), adult mouse kidney membranes (50 μg protein) or mouse urine samples (40-μl aliquots; see below) were incubated overnight at 37°C in the absence or presence of 1 U peptide-N-glycosidase F (PNGase F) according to the manufacturer's instructions (Roche Molecular Biochemicals, Mannheim, Germany).

Proteins were analysed by SDS-PAGE (7.5%) and transferred to poly(vinylidene difluoride) membranes (Millipore, Belford, Mass., USA; pore size: 0.45 μm) by standard procedures (Corbeil et al. 2001a). Immunoblotting was performed essentially as described by Corbeil et al. (2001a) with, as primary antibody, either rabbit αE3 antiserum (1:3,000) against prominin-2 (Fargeas et al. 2003b) or rat monoclonal antibody (mAb) 13A4 (1 μg/ml) against prominin-1 (Weigmann et al. 1997) or mouse mAb anti-GFP (clones 7.1 and 13.1; 1:5,000; Roche Molecular Biochemicals) followed by horseradish-peroxidase-conjugated secondary antibody. Antigen-antibody complexes were detected by using enhanced chemiluminescence (ECL system, Amersham Biosciences) and quantified, after scanning the Hyperfilm (Amersham), by means of MacBas software.

Cell-surface biotinylation and streptavidin precipitation

Unless indicated otherwise, all steps were carried out at 4°C. Just prior to use, the membrane-impermeable sulphosuccinimidyl-6(biotinamido)-hexanoate biotinylating agent (called sulfo-NHS-LC-biotin; Pierce) was dissolved in Ca/Mg-PBS (phosphate-buffered saline containing 1 mM $CaCl_2$, 0.5 mM $MgCl_2$) to give a final concentration of 0.2 mM. After repeated washes with Ca/Mg-PBS, confluent transfected MDCK cells (on 100-mm dishes) were incubated for 1 h in 2 ml biotin solution, washed three times with Ca/Mg-PBS, incubated for 10 min with Ca/Mg-PBS containing 20 mM glycine to quench the residual biotin and lysed in ice-cold solubilization buffer I. The detergent extract was diluted tenfold with Ca/Mg-PBS. Biotinylated cell-surface proteins were then adsorbed onto streptavidin-agarose beads (Sigma). After a 2-h incubation, the beads were washed and the biotinylated proteins were eluted with Laemmli buffer at 95°C. Eluates were analysed by SDS-PAGE followed by immunoblotting.

For domain-selective cell-surface biotinylation, 5-day-old monolayers on duplicate Transwell filters were washed three times with Ca/Mg-PBS and then biotinylated from either the apical (1.5 ml) or basolateral (2.6 ml) chamber compartment. The compartment not receiving sulfo-NHS-LC-biotin was filled with Ca/Mg-PBS. After quenching, cells were lysed in ice-cold solubilization buffer I and detergent extracts were then subjected to streptavidin-agarose adsorption. Biotinylated proteins were analysed by immunoblotting as described above.

Immunofluorescence and confocal microscopy

MDCK cells that had been double-transfected with prominin-1 and prominin-2-GFP and grown as a 5-day-old monolayer on Nunc filters were washed with PBS and then fixed with 3% paraformaldehyde in PBS for 30 min at room temperature. Filters were then rinsed with and incubated for 10 min in PBS containing 50 mM ammonium chloride. Cells were permeabilized and blocked with 0.2% saponin/0.2% gelatin in PBS (blocking solution) for 30 min and then incubated sequentially for 30 min each with mAb 13A4 (10 μg/ml) and Cy3-conjugated goat anti-rat IgG (H+L; Jackson ImmunoResearch Labs, West Grove, Pa., USA) diluted in blocking solution. Primary and secondary antibodies were added to both sides of the filters. In some experiments, cells were double-labelled with mAb 13A4 and mouse mAb anti-acetylated tubulin (Sigma; clone 6-11B-1) followed by Cy5-conjugated goat anti-rat IgG and Cy3-conjugated goat anti-mouse IgG (Jackson ImmunoResearch Labs). Nuclei were stained with 4,6-diamidino-2-phenylindrole (DAPI; 1 μg/ml; Molecular Probes) for 10 min at room temperature. The filters were washed in PBS, cut out, dipped in water and mounted as previously described (Corbeil et al. 1999). The cells were observed with a Leica TCS SP2 confocal laser scanning microscope. The microscope settings were such that photomultipliers

were within their linear range. Fluorophores and GFP were excited sequentially to minimize potential cross-collection of signals. The images shown were prepared from the confocal data files by using Adobe photoshop software.

Immunoelectron microscopy

MDCK cells stably transfected with prominin-2-GFP and cultured on collagen-coated 100-mm Petri dishes (Collagen R; Serva) were washed with 0.1 M sodium phosphate buffer, pH 7.4, and fixed with 4% paraformaldehyde/0.05% glutaraldehyde in 0.1 M phosphate buffer at room temperature for 8 h and then at 4°C overnight. Fixed cells were washed with phosphate buffer and 0.1% glycine in 0.1 M phosphate buffer for 5 min, scraped off the dishes in 10% gelatine in 0.1 M phosphate buffer and centrifuged for 10 min at 2,430*g*. The resulting gelatine pellet was cut into small pieces on ice and infiltrated in 2.3 M sucrose in 0.1 M phosphate buffer. The sucrose-infiltrated samples were cryosectioned on a Leica UltracutUCT microtome fitted with an FCS cryochamber (Leica Microsystems, Bensheim). Sections were retrieved by using a 1:1 mixture of 2% methyl cellulose/2.3 M sucrose. After removal of the gelatine by incubation on PBS at 37°C, sections were labelled with goat-anti-EGFP antibody (15 ng/μl; a gift from David Drechsel, MPI-CBG) followed by secondary antibody coupled to 10-nm gold (British Biocell). The sections were contrasted with a mixture of 1.9% methyl cellulose/0.3% uranyl acetate for 10 min on ice and observed by using a Morgagni electron microscope (FEI Company, Eindhoven, Netherlands).

Scanning electron microscopy

Prominin-1-transfected MDCK cells grown as a 5-day-old monolayer on glass coverslips were fixed with 2% glutaraldehyde in 0.15 M sodium phosphate buffer, pH 7.4, at room temperature for 1 h and then at 4°C overnight. Fixed cells were dehydrated in ascending concentrations of acetone (30%, 50%, 70%, 90% and 100%) and subjected to critical-point drying by using liquid carbon dioxide (CPD 030; BAL-TEC, Witten, Germany). Coverslips were mounted on aluminium stubs, coated with gold in a sputter coater (SCD 050; BAL-TEC) and observed with a scanning electron microscope (XL 30 ESEM FEG; FEI Company).

Photo-cholesterol labelling

The preparation of the [^{3}H]photocholesterol-methyl-β-cyclodextrin ([^{3}H]Ch-mβCD) inclusion complex and the photoaffinity labelling of prominin-2-GFP-transfected MDCK cells were performed as described previously (Thiele et al. 2000); cells were grown in 100-mm dishes and labelled for 14 h with 10 ml lipid-free medium containing 100 μl [^{3}H]Ch-mβCD (0.4 mCi [^{3}H]photocholesterol, 2.5 mg methyl-β-cyclodextrin) complex. After ultraviolet (UV) irradiation, cells were lysed in solubilization buffer II (1% Triton X-100, 0.5% deoxycholate, 150 mM NaCl, 50 mM TRIS-HCl, and protease inhibitors) and prominin-2-GFP was immunoprecipitated from a detergent extract obtained after centrifugation (10 min, 10,000*g*) by using mAb anti-GFP as described previously (Corbeil et al. 1999). Immunoprecipitated prominin-2-GFP and total detergent extract were analysed by SDS-PAGE followed by fluorography.

Detergent lysis and differential centrifugation

Pellets (7 μl) of prominin-2-GFP-transfected MDCK cells were lysed giving ~1.5 mg protein per milliliter for 30 min on ice in 70 μl ice-cold buffer A (150 mM NaCl, 2 mM EGTA, 50 mM TRIS-HCl pH 7.5, 10 μg ml^{-1} aprotinin, 2 μg ml^{-1} leupeptin and 1 mM PMSF; Röper et al. 2000) containing either 0.5% Triton X-100 or 0.5% Lubrol WX (Lubrol 17A17, Serva). In some experiments, solubilization was performed at 37°C instead of 4°C. Cell lysates were centrifuged at 4°C either for 10 min at 17,000*g* or for 1 h at 100,000*g*. The entire supernatant and pellet were analysed by SDS-PAGE followed by immunoblotting with mouse mAb anti-GFP.

Detergent lysis and sucrose flotation gradients

Pellets (~50 μl) of prominin-2-GFP-transfected MDCK cells were lysed giving ~3.5 mg protein per milliliter for 30 min on ice in 200 μl ice-cold buffer A containing one of 0.5% Triton X-100, 0.5% Lubrol WX, 20 mM CHAPS (AppliChem) or 0.5% Brij 58 (Sigma). The resulting detergent lysate (250 μl) was brought to 1.2 M sucrose by using 2.4 M sucrose in buffer A, placed at the bottom of a SW60 tube and overlaid with 1 ml 0.9 M sucrose, 0.5 ml 0.8 M sucrose, 1 ml 0.7 M sucrose and 1 ml 0.1 M sucrose in buffer A as described previously (Röper et al. 2000). Samples were centrifuged at 4°C for 14 h at 335,000*g*. After centrifugation, 500-μl fractions were collected from the top to the bottom of the gradient by using a pipette, the pellet was resuspended in 500 μl buffer A containing 1% Triton X-100, and 450-μl aliquots of each fraction were concentrated by methanol/chloroform (2:1) precipitation and analysed by SDS-PAGE followed by immunoblotting. The remaining 50-μl aliquot of each fraction was used to determine the sucrose concentration by measuring the refractive index.

Methyl-β-cyclodextrin treatment

Pellets (~50-μl) of prominin-2-GFP-transfected MDCK cells were resuspended in 200 μl ice-cold buffer A containing 5 mM mβCD (Sigma) and incubated for 30 min at 4°C with occasional agitation. Cholesterol-depleted cells were then

centrifuged for 1 h at 100,000*g*, lysed and subjected to a sucrose density gradient as described above.

Isolation of prominin-containing membrane particles

From double-transfected MDCK cultures

MDCK cells double-transfected with prominin-1 and prominin-2-GFP cDNA constructs and grown as 4-day-old monolayers on Transwell filter were given fresh complete culture medium (apical, 1.5 ml; basolateral, 2.6 ml). After 24 h, the media were collected from both chambers and subjected to differential centrifugation as follows (all steps at 4°C): 5 min at 300*g*; supernatant, 20 min at 1,200*g*; supernatant, 30 min at 10,000*g*; supernatant, 1 h at 200,000*g*; supernatant, 1 h at 400,000*g*. The resulting pellets were resuspended in SDS sample buffer and analysed by immunoblotting for prominin-1 and prominin-2-GFP by using either rat mAb 13A4 or mouse mAb anti-GFP, respectively. Proteins in the 400,000*g* supernatant were concentrated by methanol/chloroform (2:1) precipitation and analysed in parallel.

For the immunofluorescence analysis of prominin-containing membrane particles in the medium, transfected MDCK cells grown in 80-mm dishes were given fresh serum-free medium, which was collected after 24 h (conditioned medium). The conditioned medium was centrifuged for 30 min at 10,000*g* and the resulting supernatant (6 ml) was concentrated into 200 μl by using Centricon PL-30 (Millipore). The sample was diluted with PBS (1:1) and spotted onto a polylysine-coated glass coverslip for 30 min at room temperature. The absorbed particles were fixed with 4% paraformaldehyde in PBS for 10 min at room temperature, quenched with 50 mM ammonium chloride and subjected to immunofluorescence analysis as described above.

For the immunoprecipitation of prominin-containing membrane particles, the conditioned medium was centrifuged for 30 min at 10,000*g* and the resulting supernatant was divided in two aliquots (2 ml each). MAb 13A4 (10 μg) was added to one aliquot; both samples were then incubated overnight at 4°C end-over-end. The immune complexes were collected with Protein-G Sepharose beads (GE Healthcare Biosciences, Uppsala, Sweden). After a 3-h incubation at 4°C, the beads were washed five times with cold PBS; 10% of the beads were mounted in Mowiol 4.88 on a glass slide for GFP fluorescence analysis, whereas the remaining beads were analysed by immunoblotting for prominin-1 and prominin-2-GFP with either rat mAb 13A4 or mouse mAb anti-GFP, respectively.

From mouse urine

Urine samples were colleted from 8-week-old to 12-week-old female C57Bl6 mice. Complete protease inhibitor cocktail tablets were immediately added according to the manufacturer's instructions (Roche Molecular Biochemicals). Aliquots (200 μl) were subjected to differential centrifugation as described above for the MDCK culture medium, followed by immunoblotting of the resulting pellets for prominin-1 and prominin-2 with either rat mAb 13A4 or rabbit αE3 antiserum.

Results

Expression and characterization of prominin-2 in MDCK cells

To study the cellular and molecular properties of prominin-2, we established an MDCK epithelial cell line expressing mouse prominin-2. The expression of the transgene was monitored by immunoblotting with the rabbit αE3 antiserum (Fargeas et al. 2003b). The apparent molecular masses of the native and N-deglycosylated forms of prominin-2 expressed in MDCK cells were similar to those of endogenous prominin-2 associated with mouse kidney membranes (see Fig. 1a, lanes 1–4), i.e. ~115 kDa (arrowhead) and 88 kDa (arrow), respectively. Several additional, cross-reacting unglycosylated αE3-immunoreactive bands were detected in both kidney membranes and MDCK cells transfected with vector DNA alone (Fig. 1a, lanes 2 and 6, diamonds). The identity of these proteins is unknown.

Cell surface labelling with membrane impermeant sulfo-NHS-LC-biotin followed by streptavidin-agarose precipitation and immunoblotting with αE3 antiserum revealed that the recombinant prominin-2 expressed in MDCK cells was located at the cell surface. PNGase F treatment converted the N-glycosylated 115-kDa form of prominin-2 (Fig. 1b, lane 1, arrowhead) into the 88-kDa product (Fig. 1b, lane 2, arrow), in agreement with our previous experiments (Fig. 1a). In addition, an endogenous cross-reacting unglycosylated αE3-immunoreactive protein with a molecular mass of ~100 kDa was detected at the surface of the MDCK cells (Fig. 1b, lanes 1, 2, 5 and 6, diamonds). This protein was used as an internal control in our subsequent experiments.

Accumulation of prominin-2 not only in apical, but also in basolateral plasma membrane protrusions of polarized MDCK cells

To determine the distribution of prominin-2 with regard to the apical versus basolateral plasma membrane domain of epithelial cells, confluent prominin-2-transfected MDCK cells grown on Transwell filters were biotinylated with sulfo-NHS-LC-biotin on either the apical or basolateral surface. Detergent extracts were incubated with streptavi-

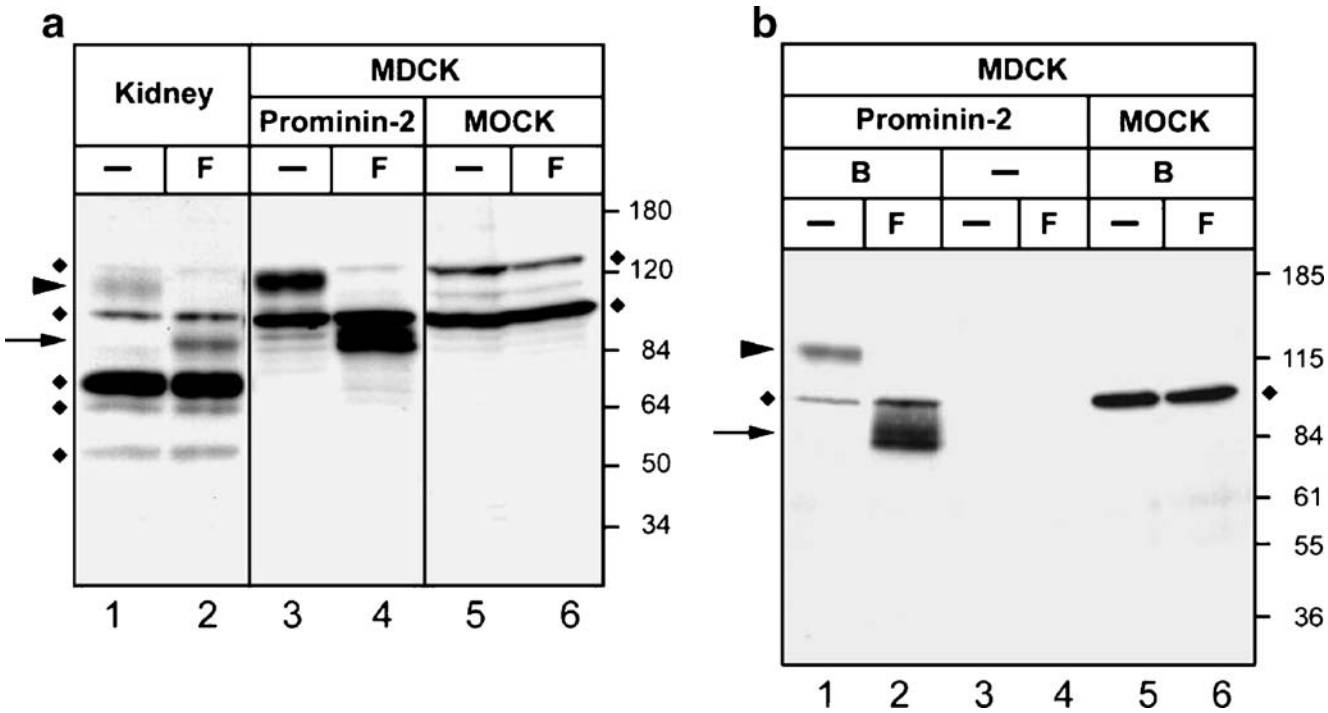

Fig. 1 Establishment of an MDCK cell line expressing prominin-2. **a** Lysates from MDCK cells stably transfected with either the expression vector containing the mouse prominin-2 cDNA (*Prominin-2*) or, as a control, vector DNA alone (*MOCK*) and, for comparison, from adult mouse kidney membrane (*Kidney*) were incubated in the absence (−) or presence (*F*) of 1 U PNGase F and analysed by immunoblotting with αE3 antiserum (*arrowhead* glycosylated prominin-2, *arrow* product after N-deglycosylation, *diamonds* immunoreactive bands of unknown identity). **b** Stably transfected MDCK cells were incubated for 1 h at 4°C without (−) or with (*B*) sulfo-NHS-LC-biotin and solubilized. Biotinylated proteins were absorbed to streptavidin-agarose beads followed by immunoblotting of the absorbed material with the αE3 antiserum (*arrowhead* glycosylated prominin-2, *arrow* product after N-deglycosylation, *diamonds* 100-kDa unknown protein). The position of prestained apparent molecular mass markers (in kDa) is indicated in **a**, **b** (*right*)

din-agarose to precipitate biotinylated surface proteins selectively; the absorbed material was analysed by SDS-PAGE followed by immunoblotting with αE3 antiserum (Fig. 2a). The 115-kDa prominin-2 band was detected in both apical and basolateral plasma membrane domains (Fig. 2a, lanes 1 and 2, arrowhead). Densitometric scanning indicated an almost equal distribution of prominin-2 between these plasma membrane domains (Fig. 2b). In contrast, our internal control, i.e. the endogenous 100-kDa protein (see above), was found predominantly in the basolateral domain (Fig. 2a,b), indicating that the MDCK cell monolayers used in our assay were fully polarized.

Immunoreactivity towards proteins other than prominin-2 by the αE3 serum precluded its use for immunofluorescence analysis. Therefore, to assess further the distribution of prominin-2 between the lateral and basal plasma membrane domain of epithelial cells, we stably transfected MDCK cells with a rat prominin-2-GFP fusion protein cDNA construct (Fargeas et al. 2003b) in which GFP was fused to the cytoplasmic C-terminal domain of prominin-2 and analysed its distribution by confocal laser scanning microscopy (CLSM). Biochemical analyses of the 142-kDa prominin-2-GFP fusion protein, which were performed along the same lines as described for the untagged mouse prominin-2 (Figs. 1, 2a), revealed that the fusion protein was (1) N-glycosylated, (2) located at the cell surface and (3) distributed in an unpolarized fashion between the apical and basolateral domain (Fig. 2c,d; data not shown), indicating that the GFP did not interfere with the proper folding of prominin-2 nor with its intracellular transport. CLSM analysis of MDCK cells double-transfected with prominin-2-GFP (green) and prominin-1 (red) revealed that prominin-2-GFP was located at the apical domain (Fig. 2e, x-y sections, Top) and the lateral domain (Fig. 2e, x-y sections, Middle, arrow) of the cells, in agreement with our biochemical data (Fig. 2c,d). Furthermore, the x-z section showed that prominin-2-GFP was also located on the basal side of MDCK cells (Fig. 2e, x-z section, arrowhead). In addition to its plasma membrane localization, prominin-2-GFP was also detected in cytoplasmic vesicles (Fig. 2e, x-y sections, Middle, outlined white arrowheads; data not shown). As previously reported (Corbeil et al. 1999), prominin-1 immunoreactivity was exclusively found at the apical surface of epithelial cells under the same conditions (Fig. 2e, red). The unpolarized distribution of prominin-2-GFP was also observed when

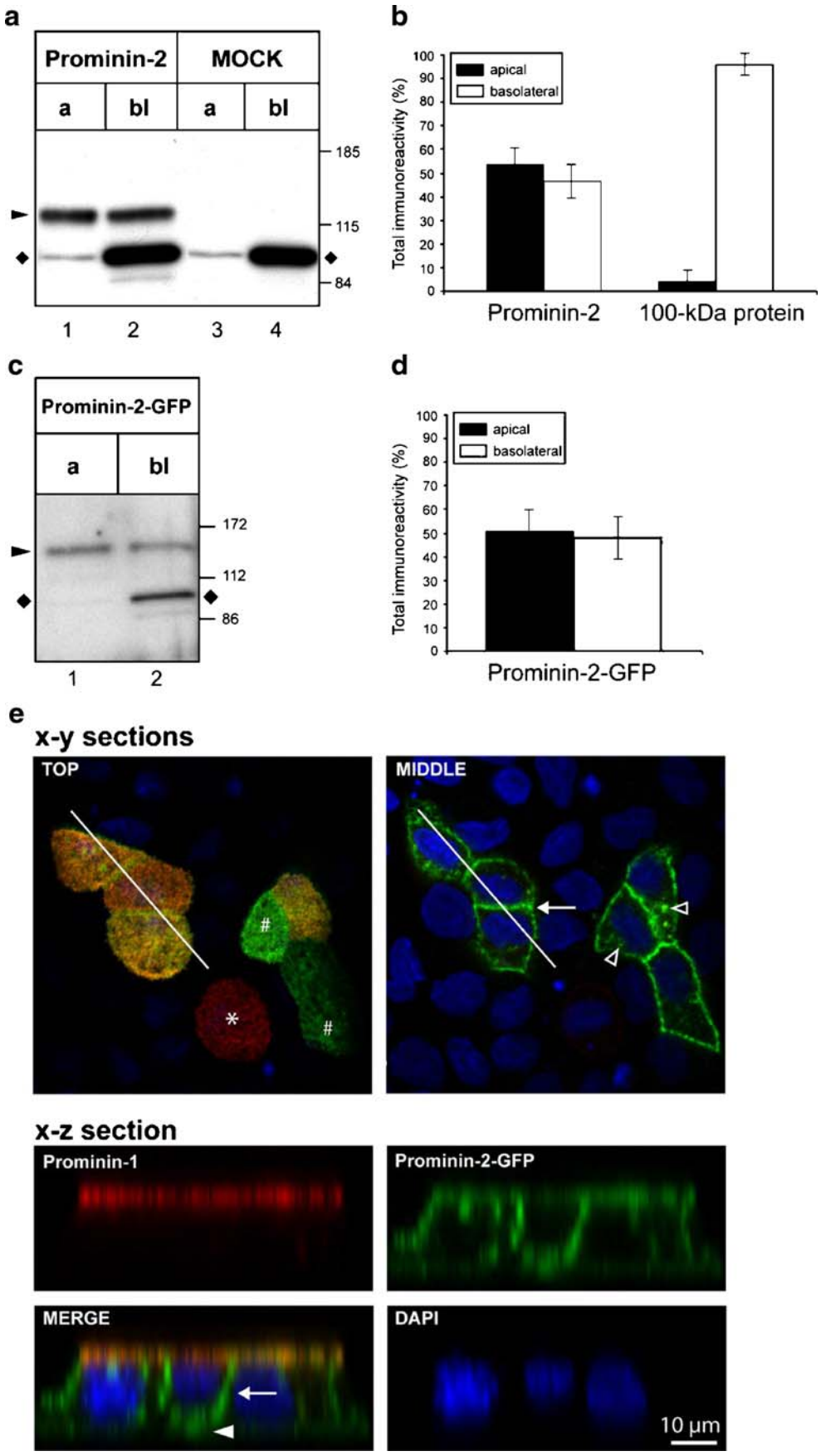

Fig. 2 Prominin-2 is found in both apical and basolateral plasma membrane domains of epithelial cells. **a** Filter-grown MDCK cells stably transfected with either the expression vector containing the mouse prominin-2 cDNA (*Prominin-2*) or, as a control, vector DNA alone (*MOCK*), were biotinylated from either the apical (*a*) or basolateral (*bl*) surface for 1 h at 4°C. Cells were solubilized and biotinylated proteins were adsorbed to streptavidin-agarose beads followed by immunoblotting of the adsorbed material with the αE3 antiserum (*arrowhead* prominin-2, *diamonds* endogenous cross-reacting 100-kDa protein). **b** The amount of protein at the apical and basolateral plasma membrane was quantified for both prominin-2 and the endogenous 100-kDa cross-reacting protein and shown as a percentage of their respective total amount (means±SD, *n*=3). **c**, **d** Plasma membrane distribution of prominin-2-GFP expressed in MDCK cells was studied in the same lines as described for the untagged prominin-2 (see **a**,**b**). **c** Immunoblot of streptavidin-agarose-adsorbed material was performed with a combination of mAb anti-GFP and αE3 antiserum (*arrowhead* prominin-2-GFP, *diamonds* endogenous cross-reacting 100-kDa protein). **d** Values are given as means±SD (*n*=6). **e** MDCK cells double-transfected with rat prominin-2-GFP and mouse prominin-1 were analysed for the expression of prominin-2-GFP (*green*) and immunostaining of prominin-1 (*red*). Nuclei were stained with DAPI (*blue*). *x-y sections* Single optical x-y-plane sections at the apex (*Top*) or middle (*Middle*) of the cells (*asterisk* cell expressing only prominin-1, *hatches* cells expressing only prominin-2-GFP, *open white arrowheads* intracellular prominin-2-GFP-positive vesicles). *x-z section* Single optical x-z-plane section as indicated (*top*) by the *white lines* (*arrows* lateral domain, *arrowhead* basal domain)

cells were pre-incubated with or without 2 mM sodium butyrate (instead of 5 mM), suggesting that the over-induction of the transgene did not lead to its miss-sorting (data not shown). Taken together, the biochemical and morphological data revealed the unpolarized distribution of prominin-2 in epithelial cells, in strong contrast with the exclusively apical localization of prominin-1 (Corbeil et al. 1999; Weigmann et al. 1997).

The punctate pattern of prominin-2-GFP staining observed at the apical domain of polarized epithelial cells (Fig. 2e, x-y sections, Top, hatch), a characteristic of a microvilli-associated antigen, indicated that prominin-2 might be associated with various types of plasmalemmal protrusions, as previously reported for prominin-1 (Corbeil et al. 1999; Weigmann et al. 1997). Indeed, a single optical x-y-plane section at the cell zenith revealed that prominin-2-GFP, like prominin-1 (V. Dubreuil et al., manuscript under revision), was also found in cilia (revealed with anti-acetylated tubulin antibody) essentially at the bulging tip (Fig. 3a, arrow). Scanning electron microscopy of a cilium present at the apical domain of the MDCK cells corroborated this morphology (Fig. 3b, arrow). Both prominin molecules were also observed in various long (10—15 μm) and thick (0.2—1 μm), acetylated tubulin-positive structures located at the apical domain (Fig. 3c,d). Some of these structures emerging from two distinct cells that appeared to be connected (Fig. 3c, Ac Tubulin, inset). Whereas it remains uncertain whether these are relics of incomplete cytokinesis, prominin-1 has been found to be concentrated at the midbody of neuroepithelial cells (V. Dubreuil et al., manuscript under revision). Prominin molecules seem to be dispensable for the formation of such protuberances, since they are found in prominin-negative cells (Fig. 3e,f; data not shown). Scanning electron microscopy confirmed the presence of long protuberances at the apical plasma membrane domain (Fig. 3g,h). Finally, a single optical x-y-plane section at the level of the basal membrane revealed that prominin-2-GFP was localized in the microspikes found therein (Fig. 3i, arrowheads).

The predominant prominin-2-GFP-labelled structures of the plasma membrane, in electron-microscopic experiments, were protrusions, irrespective of the origin of their plasma membrane domain (Fig. 4). At the apical domain, prominin-2-GFP was confined to the cilium (Fig. 4a, asterisk) and microvilli (Fig. 4a) and no significant labelling could be detected in the neighbouring planar areas (Fig. 4a, arrowheads). At the lateral domain, prominin-2-GFP was concentrated in interdigitated processes between adjacent cells (Fig. 4b, arrows). Although the MDCK cells showed few plasma membrane protrusions at their basal side, prominin-2-GFP appeared to be concentrated in some of them (Fig. 4c) in agreement with the CLSM data. Prominin-2-GFP immunoreactivity was less abundant at the basal domain than at the apical and lateral plasma membrane domains.

Prominin-2: a cholesterol-binding protein

Given the property of prominin-1 to bind plasma membrane cholesterol (Röper et al. 2000), we investigated whether prominin-2 also interacted directly with cholesterol. We incubated prominin-2-GFP-transfected MDCK cells with [^{3}H]photocholesterol, a photoactivable radioactive derivative of cholesterol (Thiele et al. 2000). Following UV irradiation, the total cell lysate and prominin-2-GFP immunoprecipitated therefrom were analysed by SDS-PAGE followed by fluorography (Fig. 5). Analysis of the total cell lysate showed that, under our conditions, a discrete set of proteins was labelled with [^{3}H]photocholesterol (Fig. 5, bottom panel, lane 1, arrows), one of these having been previously identified as the 21-kDa cholesterol-interacting protein caveolin (Fig. 5, bottom panel, lane 1, diamond). The pattern of [^{3}H]-labelled proteins was distinct from that of the proteins detected by cell-surface biotinylation (see below), suggesting that only a particular group of proteins interacted with membrane cholesterol. As a control, no labelling was observed without UV irradiation (Fig. 5, bottom panel, lane 2). Interestingly, the prominin-2-GFP immunoprecipitate revealed that prominin-2 and cholesterol directly interacted with each other (Fig. 5, top panel, lane 1, arrowhead). No such signal was detected when MDCK cells were transfected with the expression vector alone (Fig. 5, top panel, lane 3).

Partial association of prominin-2 with detergent-resistant membranes

We next investigated whether prominin-2 was associated with cholesterol-based lipid microdomains as previously shown for prominin-1 (Röper et al. 2000). As lipid microdomains had been previously characterized by their insolubility in non-ionic detergents in the cold, notably in Triton X-100 (Fiedler et al. 1993; Melkonian et al. 1995), we solubilized confluent prominin-2-GFP-transfected MDCK cells in 0.5% Triton X-100 in the cold and fractionated the lysates into detergent-soluble and -insoluble material, which were then analysed by immunoblotting. Prominin-2-GFP was found to be completely soluble in Triton X-100 after centrifugation for 10 min at 17,000*g* (Fig. 6a, lane 1) or 1 h at 100,000*g* (Fig. 6a, lane 3), as reported previously for prominin-1 (Röper et al. 2000). The same data were obtained with the untagged prominin-2 (data not shown). To investigate further a putative interaction of prominin-2-GFP with lipid microdomains, we decided to explore other solubilization conditions that might preserve such association (Röper et al. 2000).

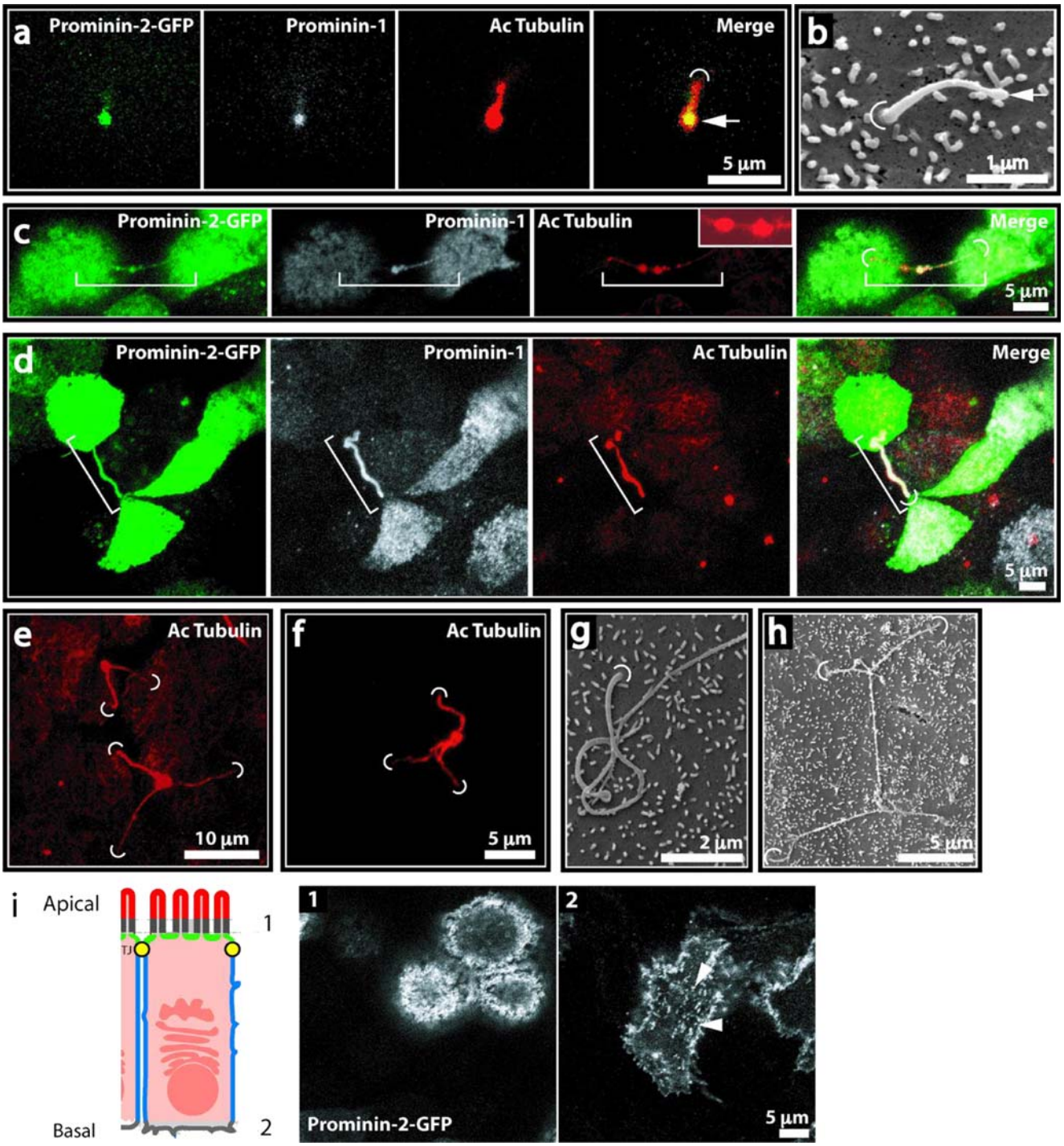

Fig. 3 Prominin-2 is found in various plasma membrane protrusions. MDCK cells double-transfected with rat prominin-2-GFP and mouse prominin-1 cDNAs were analysed for the expression of prominin-2-GFP (*green*) and immunostained for prominin-1 (*white*) and acetylated tubulin (*Ac tubulin*, *red*). **a** Single optical x-y-plane section at the cell zenith. Note that prominin-2-GFP, like prominin-1, is enriched at the cilium tip (*arc* origin of cilium, *arrow* cilium tip). **b** Scanning electron micrograph of the apical plasma membrane of MDCK cells (*arc* origin of cilium, *arrow* cilium tip). **c–e** Series of optical x-y-plane sections at the level of the apex of the cells (*arcs* origins of cilia). *Inset* in **c** Acetylated tubulin structures are connected (*brackets* apical plasma membrane protrusions). **g**, **h** Scanning electron micrographs of the apical plasma membrane of MDCK cells (*arcs* origins of cilia). **i** Single optical x-y-plane sections at the level of the apical (*1*) and basal membrane (*2*). Note the microspikes present at the basal membrane (*arrowheads*)

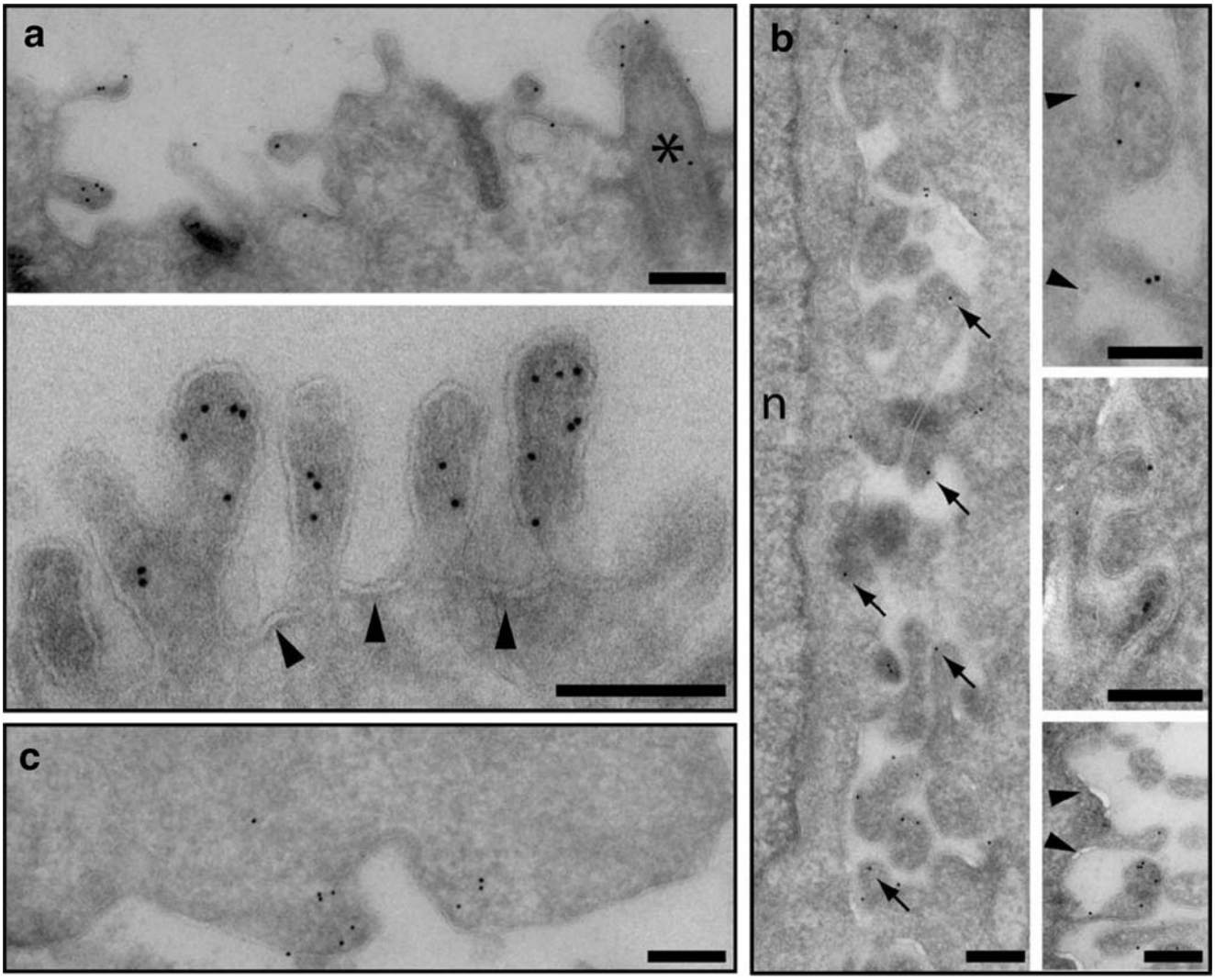

Fig. 4 Immunoelectron microscopy of prominin-2-GFP on the apical and basolateral plasma membrane domains. Ultrathin cryosections of prominin-2-GFP-transfected MDCK cells were stained with goat-anti-GFP antiserum followed by rabbit-anti-goat IgG coupled to 10-nm gold particles. **a** Apical plasma membrane domain of polarized MDCK cells. Prominin-2-GFP immunoreactivity is confined to cilium (*top*) and microvilli (*asterisk* cilium, *arrowheads* intermicrovillar regions). **b**, **c** Lateral and basal plasma membrane domains, respectively, of polarized MDCK cells. Prominin-2-GFP immunoreactivity is observed in various plasma membrane protrusions (*arrows* lateral protrusions, *n* nucleus, *arrowheads* non-protruding regions devoid of prominin-2-GFP). *Bars* 200 nm. Note that the gold particles lie at the cytoplasmic side of the cells, in agreement with the cytoplasmic localization of the C-terminal domain of prominin-2 (Fargeas et al. 2003b)

Interestingly, prominin-2-GFP was found to be partly insoluble at 4°C in 0.5% Lubrol WX, another non-ionic detergent (Fig. 6a, lanes 5-8). Upon centrifugation for 10 min at 17,000*g*, 36±4% (*n*=5) of prominin-2-GFP was sedimented (Fig. 6b, 17 K), whereas upon centrifugation for 1 h at 100,000*g*, 55±7% (*n*=5) of prominin-2-GFP was pelleted (Fig. 6b, 100 K). The latter result suggested that a certain proportion of prominin-2 molecules that were recovered in the supernatant after centrifugation for 10 min at 17,000*g* (~20%) were not truly soluble but corresponded to small detergent-insoluble membranes. Similar results were obtained either when the cells were lysed at a protein concentration of 0.75 mg (rather then 1.5 mg) per milliliter (data not shown) or when higher concentrations of Lubrol WX were used (Fig. 6c). Domain-specific cell-surface biotinylation of transfected MDCK cells growing on Transwell filters prior to solubilization in Lubrol WX and differential centrifugation revealed no correlation between the association of prominin-2-GFP with detergent-resistant membranes and its localization in the apical versus basolateral domains (data not shown).

We and others have previously demonstrated that Lubrol-WX-resistant membranes float in a sucrose density gradient (Drobnik et al. 2002; Röper et al. 2000; Slimane et al. 2003; Vetrivel et al. 2005; Vinson et al. 2003). Therefore, if prominin-2 is associated with Lubrol-WX-

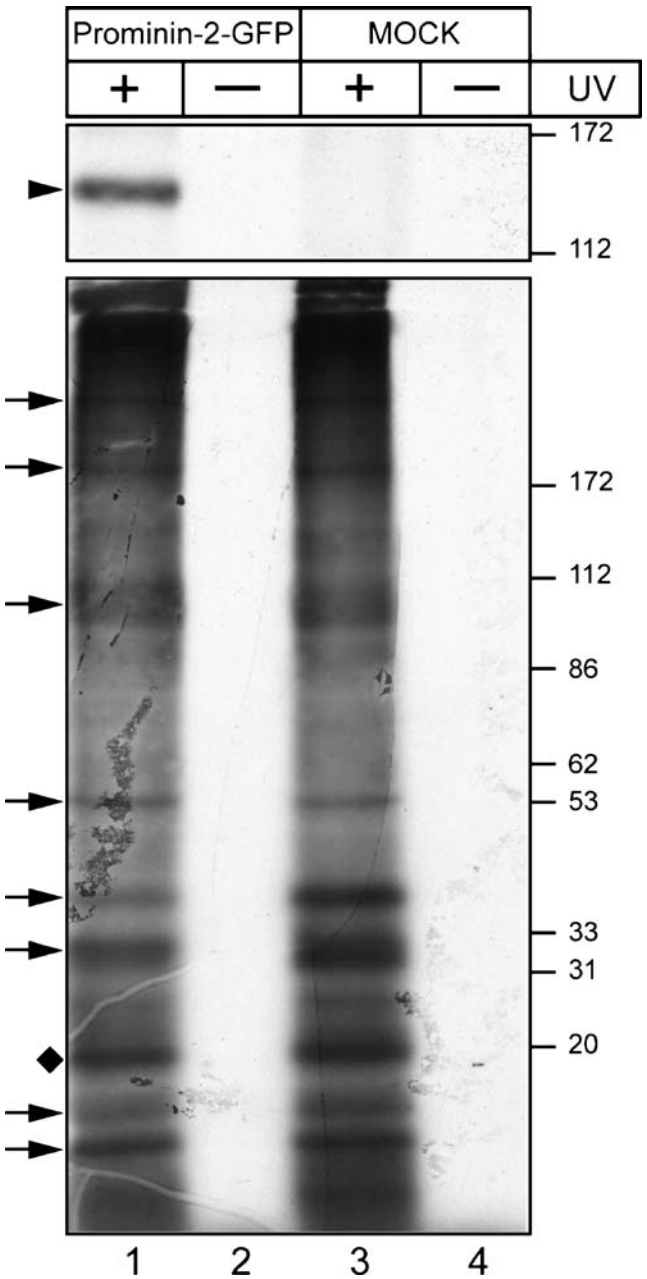

Fig. 5 Prominin-2 binds to plasma membrane cholesterol. MDCK cells stably transfected with either the expression vector containing the prominin-2-GFP cDNA (*Prominin-2-GFP*) or, as control, vector DNA alone (*MOCK*), were incubated for 14 h in the presence of [^{3}H] photocholesterol and subjected to UV irradiation (+) or kept in the dark (−). The total cell detergent extract (*bottom*) and prominin-2-GFP immunoprecipitated therefrom (*top*) were analysed by SDS-PAGE followed by fluorography (*arrowhead* prominin-2-GFP, *diamond* caveolin, *arrows* unidentified cholesterol-binding proteins)

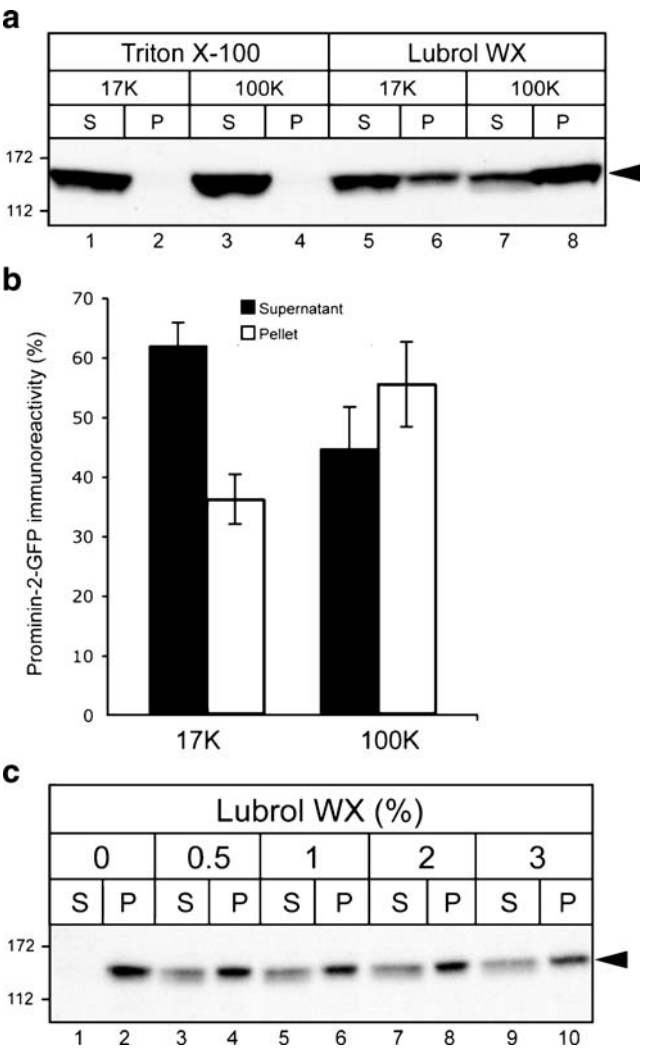

Fig. 6 Prominin-2 is associated with detergent-resistant membranes. **a** MDCK cells stably transfected with an expression vector containing the prominin-2-GFP cDNA were lysed at 4°C in either 0.5% Triton X-100 or 0.5% Lubrol WX and centrifuged either for 10 min at 17,000*g* (*17 K*) or for 1 h at 100,000*g* (*100 K*). The resulting supernatant (*S*) and pellet (*P*) were analysed by immunoblotting with αGFP antibody (*arrowhead* prominin-2-GFP). **b** After solubilization in 0.5% Lubrol WX, the amount of prominin-2-GFP immunoreactivity found in the supernatant and the pellet of both centrifugations (*17 K*, *100 K*) was quantified and shown as a percentage of the total amount (mean ± SD, *n*=5). **c** Prominin-2-GFP-transfected MDCK cells were lysed at 4°C in ice-cold solubilization buffer containing various concentrations of Lubrol WX (%) or without detergent (*0*) and centrifuged for 1 h at 100,000*g*. The resulting supernatant (*S*) and pellet (*P*) were analysed by immunoblotting with αGFP antibody (*arrowhead* prominin-2-GFP)

resistant membranes, it should float in a sucrose density gradient. Indeed, when a Lubrol WX lysate of prominin-2-GFP-transfected MDCK cells was analysed by using a flotation equilibrium sucrose density gradient, 10%–25% (mean=19.2%, *n*=6) of prominin-2-GFP was found in the low-density fractions 3–5 (Fig. 7a, panel 0.5% Lubrol WX, arrowhead). The prominin-2-GFP floating to fractions 3–5 presumably corresponded to the prominin-2-GFP associated with the large Lubrol WX-resistant membranes sedimented after centrifugation for 10 min at 17,000*g* (Fig. 6a, lane 6). Consistent with this interpretation, prominin-2-GFP recovered in the pellet fraction after centrifugation for 10 min at 17,000*g* was found to be enriched in fractions 3–

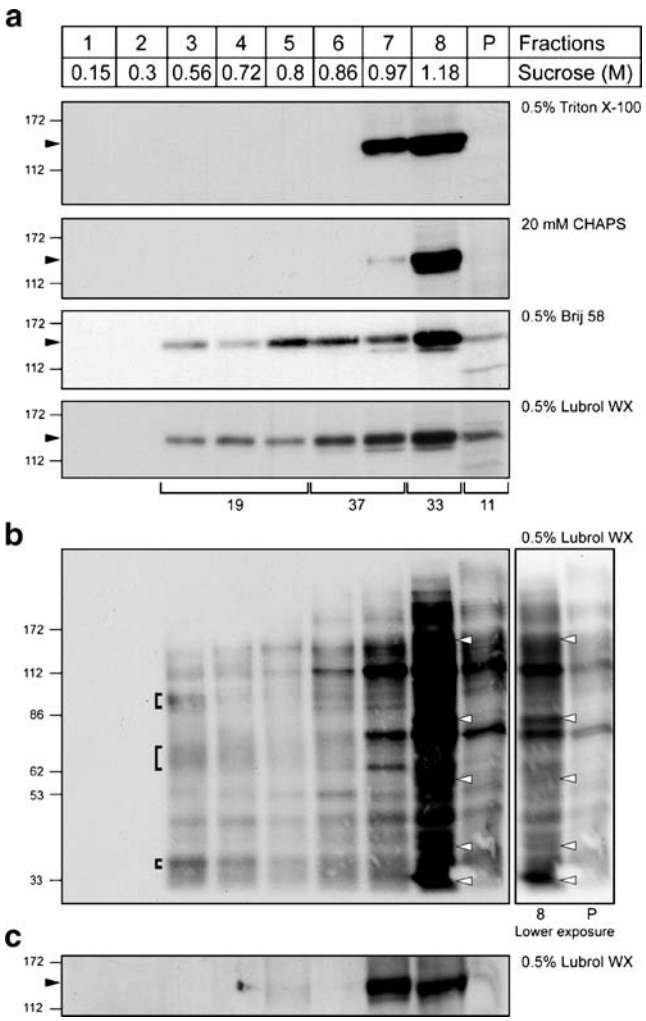

Fig. 7 Characterization of detergent-resistant membranes containing prominin-2-GFP. **a** Prominin-2-GFP-transfected MDCK cells were lysed at 4°C in either 0.5% Triton X-100, 20 mM CHAPS, 0.5% Brij 58 or 0.5% Lubrol WX. The cell lysates were subjected to flotation on a sucrose density step gradient. Equal volumes of the recovered fractions were analysed by immunoblotting with αGFP antibody (*arrowhead* prominin-2-GFP, *numbers bottom* mean of prominin-2-GFP immunoreactivy observed in the corresponding fraction; n=6). **b** Confluent prominin-2-GFP-transfected MDCK cells were cell-surface-biotinylated for 1 h at 4°C prior to solubilization in 0.5% Lubrol WX and subjected to flotation on a sucrose density step gradient. Equal volumes of the recovered fractions were analysed by NeutrAvidin blotting (*brackets* insoluble-floating proteins, *arrowheads* soluble proteins completely recovered in loading fraction). **c** Prominin-2-GFP-transfected MDCK cells were incubated with 5 mM mβCD at 4°C prior to solubilization in 0.5% Lubrol WX. The cell lysates were fractionated on a sucrose density step gradient. Equal volumes of the recovered fractions were analysed by immunoblotting with αGFP antibody (*arrowhead* prominin-2-GFP)

5 upon sucrose density gradient centrifugation (data not shown). Similar results were obtained by using the detergent Brij 58 instead of Lubrol WX (Fig. 7a), whereas upon solubilization in Triton X-100 or the zwitterionic detergent CHAPS, prominin-2-GFP was recovered in the bottom fractions 7 and 8 of the flotation gradient (Fig. 7a), with fraction 8 corresponding to the load. These data agreed with the complete solubility of prominin-2-GFP in these detergents (Fig. 6a; data not shown). The significant proportion of prominin-2-GFP associated with the fractions of greater buoyant density (fractions 7 and 8) upon Lubrol WX solubilization (Fig. 7a) might have corresponded, at least partly, to the soluble fraction of prominin-2-GFP recovered in the supernatant after centrifugation for 1 h at 100,000*g* (Fig. 6a, lane 7). The small fraction of prominin-2-GFP (~20%) associated with the small detergent-resistant membranes recovered after centrifugation for 1 h at 100,000*g*, but not for 10 min at 17,000*g*, might have been contained in fractions 6 and 7, as previously shown for prominin-1 (Röper et al. 2000).

Based on the arguments of Schuck et al. (2003) and Shogomori and Brown (2003), the partial insolubility of prominin-2 in Lubrol WX, as revealed by its sedimentation (Fig. 6) and its floatation upon density gradient centrifugation (Fig. 7a), might simply have been a reflection of Lubrol WX being a milder non-ionic detergent than Triton X-100 (Schuck et al. 2003), rather than revealing the existence of specific (Triton-X-100-soluble but Lubrol WX-insoluble) subpopulations of membrane microdomains. To address this issue, we performed cell-surface biotinylation on confluent MDCK cells prior to detergent extraction and analysed the distribution of the biotinylated proteins across a flotation equilibrium sucrose density gradient by NeutrAvidin blotting (Fig. 7b). Approximately half of the biotinylated proteins were recovered in the pellet and fraction 8 (Fig. 7b), several of them being found exclusively in fraction 8, indicating their complete solubilization (Fig. 7b, arrowheads). Interestingly, a discrete set of biotinylated proteins, distinct from the major bands in fraction 8, were selectively enriched in fractions 3–5, suggesting their specific association with Lubrol-WX–resistant membranes (Fig. 7b, brackets). These observations suggested that the partial insolubility of prominin-2-GFP in Lubrol WX was not attributable to an overall lower efficiency of Lubrol WX (compared with Triton X-100) as a detergent but reflected a specific phenomenon.

Sensitivity of Lubrol-WX-resistant membrane complexes containing prominin-2 to cholesterol depletion

Given that prominin-2 interacts with plasma membrane cholesterol (see Fig. 5), we further investigated whether cholesterol was relevant for the maintenance of its association with Lubrol-WX-resistant membrane complexes. To remove cholesterol from the plasma membrane, prominin-2-GFP-transfected MDCK cells were treated at 4°C with methyl-β-cyclodextrin (mβCD), which is known selectively to deplete biological membranes of cholesterol

(Klein et al. 1995). Scraped cells were treated with 5 mM mβCD in the cold. The cholesterol-depleted cell pellet that was recovered after centrifugation was then solubilized in 0.5% Lubrol WX. The mβCD treatment *per se* did not lead to solubilization of prominin-2-GFP (data not shown). Flotation gradient analysis of the Lubrol WX lysate revealed however that cholesterol depletion altered the flotation behaviour of prominin-2-GFP. Instead of a proportion of prominin-2-GFP floating to fractions 3–6, almost all of it moved from fraction 8 (the load) to fraction 7 (Fig. 7c).

Occurrence of prominin-2-containing particles

We recently demonstrated that prominin-1 was associated with membrane particles that were released into the culture medium of carcinoma-derived Caco-2 cells, and physiologically, into various human body fluids and mouse ventricular fluid (Marzesco et al. 2005). We now determined whether the same phenomenon occurred with respect to prominin-2. Examination of the apical and basolateral culture media by differential centrifugation followed by immunoblotting revealed the presence of prominin-2-GFP in both media (Fig. 8a, bottom panels, arrowhead) whereas prominin-1 immunoreactivity was found, as expected, only in the apical culture medium (Fig. 8a, top panels, bracket). The CLSM analysis revealed that prominin molecules recovered in the pellet fractions upon low-speed centrifugations, i.e. 300*g* and 1,200*g*, were associated with cell debris (data not shown). Interestingly, a similar analysis of the supernatant fraction obtained upon centrifugation at 10,000*g* for 30 min (a fraction that indeed contained the prominin immunoreactivity found in the 200,000*g* and 400,000 g pellet fractions; see Fig. 8a, left), showed that prominin-2-GFP and prominin-1 were associated with small particles, some of which contained both prominin molecules (Fig. 8b, arrows). Indeed, 40% of particles were positive for both prominin molecules, whereas 26% and 34% are positive for prominin-2-GFP and prominin-1 (n=301 particles), respectively. A type of particle aggregation was observed in the 10,000*g* pellet fraction (data not shown). The co-localization of both prominins in extracellular particles was further documented by immunoprecipitation. The prominin-1-containing particles, which were recovered with complexes of mAb 13A4 (anti-prominin-1 antibody) and protein-G attached to sepharose beads, exhibited GFP fluorescence indicating the presence of prominin-2-GFP (Fig. 8c). No fluorescence was observed when the primary antibody was omitted (Fig. 8c). Immunoblotting of prominin-1-containing membrane particles immunoprecipitated with mAb 13A4 confirmed the presence of both prominins, i.e. immunoreactivity for prominin-1 (Fig. 8d, left, bracket) and prominin-2-GFP (Fig. 8d, right, arrowhead).

We subsequently investigated whether prominin-2-containing particles existed physiologically. Given the strong expression of prominin-2 in adult kidney (Fargeas et al. 2003b), we examined their presence in urine. The immunoblotting of mouse urine revealed the occurrence of prominin-2 in this fluid (Fig. 8e, lanes 3 and 4). Prominin-1 was also detected (Fig. 8e, lanes 1 and 2) as previously demonstrated for its human orthologue (Marzesco et al. 2005). In this fluid, prominin-containing particles were exclusively sedimented by centrifugation for 1 h at 200,000*g* (Fig. 8f, lane 4). Prominin-2 was also co-immunoprecipitated with prominin-1-containing particles, as were those found in MDCK cell media (data not shown).

Discussion

We report five novel observations concerning prominin-2. First, prominin-2 is distributed in a non-polarized fashion between the apical and basolateral plasma membrane domains of epithelial cells. Second, irrespective of the plasma membrane domain, prominin-2 is selectively concentrated in plasma membrane protrusions. Third, it is associated with small membrane particles that are released into the extracellular milieu, such as urine. Fourth, prominin-2 binds to plasma membrane cholesterol. Fifth, prominin-2 is partly associated with detergent-resistant membranes in a cholesterol-dependent manner suggesting its incorporation into membrane microdomains.

The biochemical and morphological analyses of polarized MDCK cells expressing recombinant prominin-2 have revealed a non-polarized distribution of this membrane glycoprotein at the plasma membrane, in contrast with the exclusively apical localization of its paralogue prominin-1 (Corbeil et al. 1999; Weigmann et al. 1997). These observations suggest that either prominin-2 does not contain an apical sorting signal and thus differs from prominin-1 (Corbeil et al. 1999) or it contains both a basolateral and an apical sorting signal that compete with each other, resulting in a non-polarized distribution of the protein. Further studies are required to solve this issue. Nevertheless, the presence of N-glycans in prominin-2 indicates that carbohydrate structures, which have been proposed to act as a general apical sorting signal (Gut et al. 1998; Scheiffele et al. 1995; Urquhart et al. 2005), are insufficient to target this particular glycoprotein exclusively to the apical domain. Therefore, N-glycans should not be considered as the sole determinant for the apical localization of membrane glycoproteins, as previously suggested for soluble glycoproteins (Larsen et al. 1999; Rodriguez-Boulan and Gonzalez 1999; Trischler et al. 2001). The differential localization with respect to plasma membrane

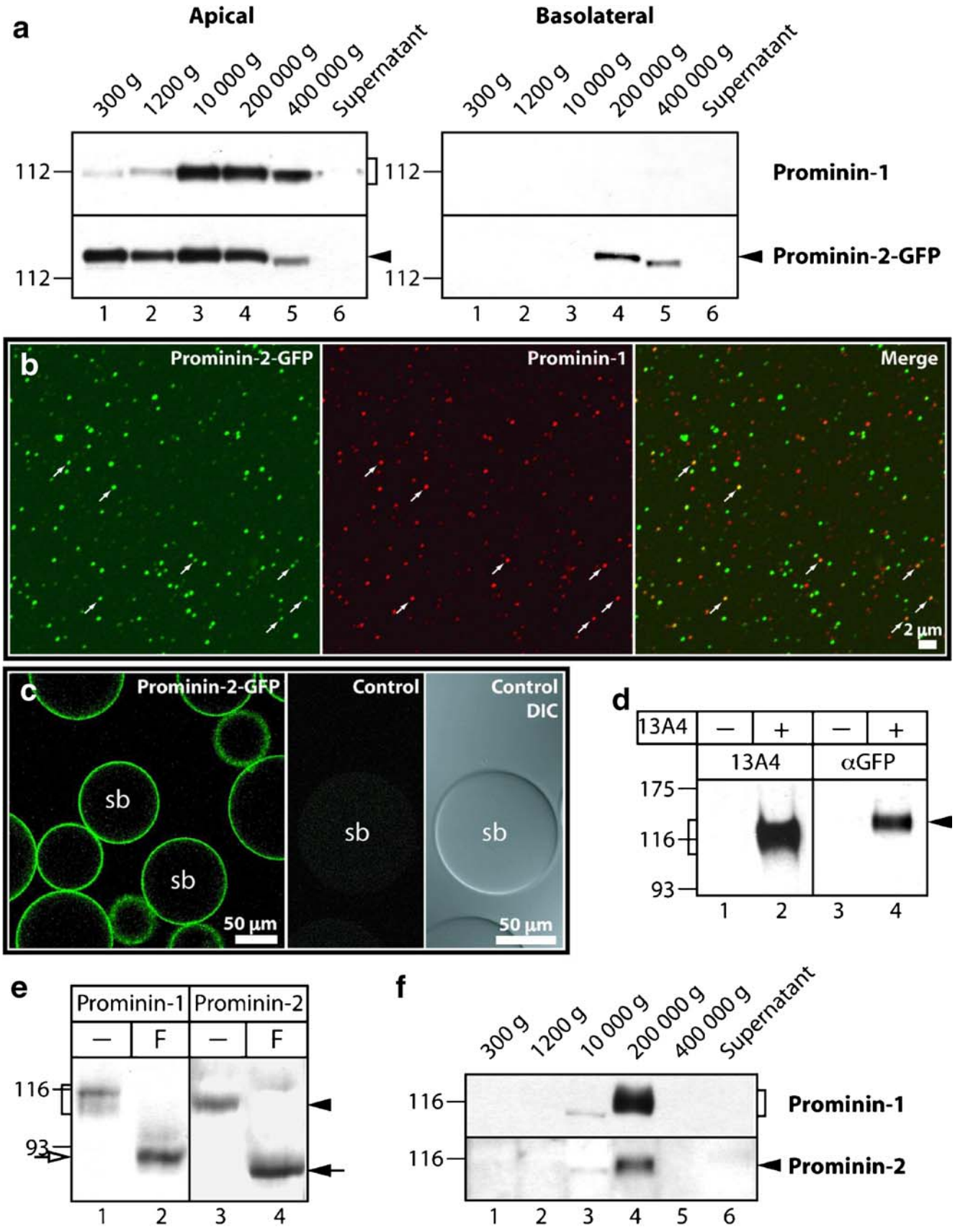
a
Apical
Basolateral
300 g
1200 g
10 000 g
200 000 g
400 000 g
Supernatant
112
Prominin-1
Prominin-2-GFP
1 2 3 4 5 6
b
Prominin-2-GFP
Prominin-1
Merge
2 µm
c
Prominin-2-GFP
Control
Control DIC
sb
50 µm
d
13A4
αGFP
175
116
93
e
Prominin-1
Prominin-2
F
f

◀ **Fig. 8** Release of extracellular particles carrying prominin-2. **a** Media conditioned for 24 h from either the upper (apical) or lower (basolateral) chamber of MDCK cells double-transfected with mouse prominin-1 and rat prominin-2-GFP cDNAs growing on filter were subjected to differential centrifugation for 5 min at 300*g*, 20 min at 1,200*g*, 30 min at 10,000*g*, 1 h at 200,000*g* and 1 h at 400,000*g*. All pellets were analysed by immunoblotting with either mAb 13A4 or αGFP antibody. Proteins in the 400,000*g* supernatant were analysed in parallel (*bracket* prominin-1, *arrowhead* prominin-2-GFP). **b** Immunofluorescence of prominin-1 and prominin-2-GFP in MDCK-derived particles present in the 10,000*g* supernatant (*arrow* particles containing both prominin molecules). Note that the particle populations that are positive either for prominin-2-GFP or prominin-1 might arise from single-transfected cells. **c**, **d** MDCK-derived particles found in the 10,000*g* supernatant were immunoprecipitated with mAb 13A4 (**c**, Prominin-2-GFP; **d**, +) or without (**c**, *Control*; **d**, −) and analysed by GFP fluorescence (**c**) on sepharose beads (*sb*) and immunoblotting (**d**, *bracket* prominin-1, *arrowhead* prominin-2-GFP) with either mAb 13A4 (*left*) or αGFP antibody (*right*). Note the lack of immunofluorescence in the control (*Control*) as revealed by differential interference contrast (*DIC*). **e** Proteins in mouse urine were incubated in the absence (−) or presence (*F*) of 1 U PNGase F and analysed by immunoblotting with either mAb 13A4 for prominin-1 or αE3 antiserum for prominin-2 (*bracket* prominin-1, *open arrow* deglycosylated prominin-1, *arrowhead* prominin-2, *arrow* deglycosylated prominin-2). **f** Mouse urine was subjected to differential centrifugation as in **a**; the resulting pellets were analysed by immunoblotting with either mAb 13A4 or αE3 antiserum (*bracket* prominin-1, *arrowhead* prominin-2)

domains of these two structurally related pentaspan membrane glycoproteins, i.e. prominin-1 (apical) and prominin-2 (apical and baso-lateral), offers an interesting cellular model for investigating the molecular determinants underlying the proper localization of polytopic membrane proteins in polarized epithelial cells. Likewise, given that prominin-2 is a cholesterol-interacting protein, these membrane proteins constitute interesting tools for identifying the amino acid residue(s) that are responsible for their interaction with plasma membrane cholesterol.

Although prominin-2 is not confined to the apical domain of polarized epithelial cells, like prominin-1, it does retain its specific sub-localization to various types of plasma membrane protrusions in all three plasmalemmal domains of polarized epithelial cells, i.e. apical, lateral and basal. Given the postulated role of prominin-1, i.e. as an organizer of certain plasma membrane protrusions (Corbeil et al. 2001b; see also below), these findings raise the interesting possibility that prominin-2 might play a similar role, particularly with regard to the protrusions associated with basal and lateral plasma membrane domains of epithelial cells, which are devoid of prominin-1 (Corbeil et al. 1999). Specifically, prominin-2 might thus functionally compensate for the loss of prominin-1 in epithelial tissues and explain why homozygous carriers of the frameshift mutation in the human *PROMININ-1* gene resulting in retinal degeneration lack other pathological symptoms (Maw et al. 2000). These interpretations are in agreement with the co-expression of prominin-2 and prominin-1 in various epithelial tissues but not in photoreceptor cells (Fargeas et al. 2003b).

Prominin-2, like prominin-1, might be involved in the maintenance of functional plasma membrane protrusions (Corbeil et al. 2001b; Jászai et al. 2006). Mechanically, prominin molecules might provide the plasma membrane outgrowths with an appropriate lipid composition, notably with respect to cholesterol, an interacting partner of both prominin molecules (see Fig. 5), and hence functionally organize plasma membrane protrusions. The association of prominin-1 (Röper et al. 2000) and prominin-2 (present study) with membrane microdomains, as defined by their detergent insolubility in a cholesterol-dependent manner, is also relevant in this context. Prominin-containing membrane microdomains might serve as building units to construct various sub-domains of the plasma membrane (e.g. microvilli, cilia, microspikes), all of which have one feature in common, i.e. they protrude from the planar regions of the plasmalemma. In agreement with this hypothesis, we and others have postulated that microvillus formation involves specific membrane lipid microdomains (Danielsen and Hansen 2003; Röper et al. 2000). Atomic force microscopy imaging has provided further support for this idea (Poole et al. 2004).

Physiologically, the concentration of such prominin-containing membrane microdomains in plasma membrane protrusions, particularly at their edge might create a phase separation with the surrounding lipid environment leading to the budding of membrane particles containing prominin molecules (Fig. 8; Marzesco et al. 2005). Since the different phases in the membrane (i.e. liquid-ordered versus liquid-disordered) modify the physical properties of the lipid bilayer, the dynamics of membrane budding may be influenced by the lipid/protein-driven formation of a specific membrane microdomain in the vicinity of the nascent bud (Huttner and Zimmerberg 2001). Consistent with this, the prominin molecules associated with the membrane particles demonstrate the same detergent solubility/insolubility and cholesterol dependence (A.-M. Marzesco et al., manuscript in preparation) as those associated with plasma membrane protrusions (present study; Röper et al. 2000). Additional investigations are needed to determine the composition (lipid and protein) of the prominin-containing membrane microdomains and the precise molecular mechanism underlying the release of prominin-containing membrane particles. Further studies are also required to determine the functional role of these membrane particles.

Finally, the partial resistance of a particular membrane protein to solubilization with non-ionic detergents, such as Triton X-100 in the cold and its association with floating detergent-resistant membranes upon density gradient cen-

trifugation, have been used to define a protein as interacting with membrane microdomains (London and Brown 2000). The use of a variety of other mild detergents, e.g. Lubrol WX and Brij 58, to determine such association has been questioned (Schuck et al. 2003; Shogomori and Brown 2003). Concerns about the ability of these detergents to solubilize membrane proteins selectively, and thus to discriminate between those associated with membrane microdomains and those not, have been raised (Schuck et al. 2003; Shogomori and Brown 2003). We have demonstrated here that Lubrol WX efficiently solubilizes the bulk of plasma membrane proteins, as previously suggested (Röper et al. 2000). Indeed, Lubrol WX extraction leads to a clear partitioning of plasma membrane proteins, with only a discrete set floating to the low-density fractions and the bulk of proteins remaining soluble (see Fig. 7b). Kuerschner and colleagues (2005) have recently observed a similar partitioning of lipids upon Lubrol WX extraction. Although Lubrol WX is "mild" compared with Triton X-100 (Schuck et al. 2003), it appears nonetheless to be a useful tool for investigating membrane microdomain association, as recently reviewed (Chamberlain 2004; Lucero and Robbins 2004).

References

Am Esch JS, Knoefel WT, Klein M, Ghodsizad A, Fuerst G, Poll LW, Piechaczek C, Burchardt ER, Feifel N, Stoldt V, Stockschlader M, Stoecklein N, Tustas RY, Eisenberger CF, Peiper M, Haussinger D, Hosch SB (2005) Portal application of autologous CD133+ bone marrow cells to the liver: a novel concept to support hepatic regeneration. Stem Cells 23:463–470

Bitan M, Shapira M, Resnick I, Zilberman I, Miron S, Samuel S, Ackerstein A, Elad S, Israel S, Amar A, Fibach E, Or R, Slavin S (2005) Successful transplantation of haploidentically mismatched peripheral blood stem cells using CD133(+)-purified stem cells. Exp Hematol 33:713–718

Bornhäuser M, Eger L, Oelschlaegel U, Auffermann-Gretzinger S, Kiani A, Schetelig J, Illmer T, Schaich M, Corbeil D, Thiede C, Ehninger G (2005) Rapid reconstitution of dendritic cells after allogeneic transplantation of CD133+ selected hematopoietic stem cells. Leukemia 19:161–165

Bussolati B, Bruno S, Grange C, Buttiglieri S, Deregibus M, Cantino D, Camussi G (2005) Isolation of renal progenitor cells from adult human kidney. Am J Pathol 166:545–555

Chamberlain LH (2004) Detergents as tools for the purification and classification of lipid rafts. FEBS Lett 559:1–5

Corbeil D, Boileau G, Lemay G, Crine P (1992) Expression and polarized apical secretion in Madin-Darby canine kidney cells of a recombinant soluble form of neutral endopeptidase lacking the cytosolic and transmembrane domains. J Biol Chem 267:2798–2801

Corbeil D, Röper K, Hannah MJ, Hellwig A, Huttner WB (1999) Selective localization of the polytopic membrane protein prominin in microvilli of epithelial cells—a combination of apical sorting and retention in plasma membrane protrusions. J Cell Sci 112:1023–1033

Corbeil D, Röper K, Hellwig A, Tavian M, Miraglia S, Watt SM, Simmons PJ, Peault B, Buck DW, Huttner WB (2000) The human AC133 hematopoietic stem cell antigen is also expressed in epithelial cells and targeted to plasma membrane protrusions. J Biol Chem 275:5512–5520

Corbeil D, Fargeas CA, Huttner WB (2001a) Rat prominin, like its mouse and human orthologues, is a pentaspan membrane glycoprotein. Biochem Biophys Res Commun 285:939–944

Corbeil D, Röper K, Fargeas CA, Joester A, Huttner WB (2001b) Prominin: a story of cholesterol, plasma membrane protrusions and human pathology. Traffic 2:82–91

Danielsen EM, Hansen GH (2003) Lipid rafts in epithelial brush borders: atypical membrane microdomains with specialized functions. Biochem Biophys Acta 1617:1–9

Drobnik W, Borsukova H, Bottcher A, Pfeiffer A, Liebisch G, Schutz GJ, Schindler H, Schmitz G (2002) Apo AI/ABCA1-dependent and HDL3-mediated lipid efflux from compositionally distinct cholesterol-based microdomains. Traffic 3:268–278

Fargeas CA, Corbeil D, Huttner WB (2003a) AC133 antigen, CD133, prominin-1, prominin-2, etc.: prominin family gene products in need of a rational nomenclature. Stem Cells 21:506–508

Fargeas CA, Florek M, Huttner WB, Corbeil D (2003b) Characterization of prominin-2, a new member of the prominin family of pentaspan membrane glycoproteins. J Biol Chem 278:8586–8596

Fargeas CA, Joester A, Missol-Kolka E, Hellwig A, Huttner WB, Corbeil D (2004) Identification of novel prominin-1/CD133 splice variants with alternative C-termini and their expression in epididymis and testis. J Cell Sci 117:4301–4311

Fargeas CA, Fonseca AV, Huttner WB, Corbeil D (2006) Prominin-1 (CD133): from progenitor cells to human diseases. Future Lipidol 1:213–225

Fiedler K, Kobayashi T, Kurzchalia TV, Simons K (1993) Glycosphingolipid-enriched, detergent-insoluble complexes in protein sorting in epithelial cells. Biochemistry 32:6365–6373

Giebel B, Corbeil D, Beckmann J, Höhn J, Freund D, Giesen K, Fischer J, Kögler G, Wernet P (2004) Segregation of lipid raft markers including CD133 in polarized human hematopoietic stem and progenitor cells. Blood 104:2332–2338

Gut A, Kappeler F, Hyka N, Balda MS, Hauri HP, Matter K (1998) Carbohydrate-mediated Golgi to cell surface transport and apical targeting of membrane proteins. EMBO J 17:1919–1929

Huttner WB, Zimmerberg J (2001) Implications of lipid microdomains for membrane curvature, budding and fission. Curr Opin Cell Biol 13:478–484

Jászai J, Fargeas CA, Florek M, Huttner WB, Corbeil D (2006) Prominin-1 (CD133). Exp Eye Res [Epub ahead of print; PMID: 16733052]

Kania G, Corbeil D, Fuchs J, Tarasov KV, Blyszczuk P, Huttner WB, Boheler KR, Wobus AM (2005) The somatic stem cell marker prominin-1/CD133 is expressed in embryonic stem cell-derived progenitors. Stem Cells 23:791–804

Klein U, Gimpl G, Fahrenholz F (1995) Alteration of the myometrial plasma membrane cholesterol content with beta-cyclodextrin modulates the binding affinity of the oxytocin receptor. Biochemistry 34:13784–13793

Kuerschner L, Ejsing CS, Ekroos K, Shevchenko A, Anderson KI, Thiele C (2005) Polyene-lipids: a new tool to image lipids. Nat Methods 2:39–45

Larsen JE, Avvakumov GV, Hammond GL, Vogel LK (1999) N-glycans are not the signal for apical sorting of corticosteroid binding globulin in MDCK cells. FEBS Lett 451:19–22

Lee A, Kessler JD, Read T-A, Kaiser C, Corbeil D, Huttner WB, Johnson JE, Wechsler-Reya RJ (2005) Isolation of neural stem cells from postnatal cerebellum. Nat Neurosci 8:723–729

London E, Brown DA (2000) Insolubility of lipids in Triton X-100: physical origin and relationship to sphingolipid/cholesterol membrane domains (rafts). Biochem Biophys Acta 1508:182–195

Lucero HA, Robbins PW (2004) Lipid rafts-protein association and the regulation of protein activity. Arch Biochem Biophys 426:208–224

Marzesco AM, Janich P, Wilsch-Bräuninger M, Dubreuil V, Langenfeld K, Corbeil D, Huttner WB (2005) Release of extracellular membrane particles carrying the stem cell marker prominin-1 (CD133) from neural progenitors and other epithelial cells. J Cell Sci 118:2849–58

Maw MA, Corbeil D, Koch J, Hellwig A, Wilson-Wheeler JC, Bridges RJ, Kumaramanickavel G, John S, Nancarrow D, Röper K, Weigmann A, Huttner WB, Denton MJ (2000) A frameshift mutation in prominin (mouse)-like 1 causes human retinal degeneration. Hum Mol Genet 9:27–34

Melkonian KA, Chu T, Tortorella LB, Brown DA (1995) Characterization of proteins in detergent-resistant membrane complexes from Madin-Darby canine kidney epithelial cells. Biochemistry 34:16167–16170

Miraglia S, Godfrey W, Yin AH, Atkins K, Warnke R, Holden JT, Bray RA, Waller EK, Buck DW (1997) A novel five-transmembrane hematopoietic stem cell antigen: isolation, characterization, and molecular cloning. Blood 90:5013–5021

Oh H, Missol-Kolka E, Moons L, Wilsch-Bräuninger M, Jansen S, Hudl K, Seeliger M, Collen D, Huttner WB, Corbeil D, Carmeliet P (2005) Prominin-1 deficiency leads to progressive retinal degeneration. ARVO 2005 Annual Meeting May 1–5, 2005, Fort Lauderdale, Florida, USA (abstract no. B421)

Poole K, Meder D, Simons K, Muller D (2004) The effect of raft lipid depletion on microvilli formation in MDCK cells, visualized by atomic force microscopy. FEBS Lett 565:53–58

Richardson GD, Robson CN, Lang SH, Neal DE, Maitland NJ, Collins AT (2004) CD133, a novel marker for human prostatic epithelial stem cells. J Cell Sci 117:3539–3545

Rodriguez-Boulan E, Gonzalez A (1999) Glycans in post-Golgi apical targeting: sorting signals or structural props? Trends Cell Biol 9:291–294

Röper K, Corbeil D, Huttner WB (2000) Retention of prominin in microvilli reveals distinct cholesterol-based lipid micro-domains in the apical plasma membrane. Nat Cell Biol 2:582–592

Scheiffele P, Peranen J, Simons K (1995) N-glycans as apical sorting signals in epithelial cells. Nature 378:96–98

Schuck S, Honsho M, Ekroos K, Shevchenko A, Simons K (2003) Resistance of cell membrane to different detergents. Proc Natl Acad Sci USA 100:5795–5800

Shogomori H, Brown DA (2003) Use of detergents to study membrane rafts: the good, the bad, and the ugly. Biol Chem 384: 1259–1293

Slimane TA, Trugnan G, Van Ijzendoorn SC, Hoekstra D (2003) Raft-mediated trafficking of apical resident proteins occurs in both direct and transcytotic pathways in polarized hepatic cells: role of distinct lipid microdomains. Mol Biol Cell 14:611–624

Thiele C, Hannah MJ, Fahrenholz F, Huttner WB (2000) Cholesterol binds to synaptophysin and is required for biogenesis of synaptic vesicles. Nat Cell Biol 2:42–49

Trischler M, Koch-Brandt C, Ullrich O (2001) Apical transport of osteopontin is independent of N-glycosylation and sialylation. Mol Membr Biol 18:275–281

Uchida N, Buck DW, He D, Reitsma MJ, Masek M, Phan TV, Tsukamoto AS, Gage FH, Weissman IL (2000) Direct isolation of human central nervous system stem cells. Proc Natl Acad Sci USA 97:14720–14725

Urquhart P, Pang S, Hooper NM (2005) N-glycans as apical targeting signals in polarized epithelial cells. Biochem Soc Symp 72:39–45

Vetrivel KS, Cheng H, Kim SH, Chen Y, Barnes NY, Parent AT, Sisodia SS, Thinakaran G (2005) Spatial segregation of gamma-secretase and substrates in distinct membrane domains. J Biol Chem 280:25892–25900

Vinson M, Rausch O, Maycox PR, Prinjha RK, Chapman D, Morrow R, Harper AJ, Dingwall C, Walsh FS, Burbidge SA, Riddell DR (2003) Lipid rafts mediate the interaction between myelin-associated glycoprotein (MAG) on myelin and MAG-receptors on neurons. Mol Cell Neurosci 22:344–352

Weigmann A, Corbeil D, Hellwig A, Huttner WB (1997) Prominin, a novel microvilli-specific polytopic membrane protein of the apical surface of epithelial cells, is targeted to plasmalemmal protrusions of non-epithelial cells. Proc Natl Acad Sci USA 94:12425–12430

Yin AH, Miraglia S, Zanjani ED, Almeida-Porada G, Ogawa M, Leary AG, Olweus J, Kearney J, Buck DW (1997) AC133, a novel marker for human hematopoietic stem and progenitor cells. Blood 90:5002–5012

Zhang Q, Haleem R, Cai X, Wang ZT (2002) Identification and characterization of a novel testosterone-regulated prominin-like gene in the rat ventral prostate. Endocrinology 143:4788–4796